Three-dimensional structure of fast ion conducting $0.5Li_2S + 0.5[(1 - x)GeS_2 + xGeO_2]$ glasses from high-energy X-ray diffraction and reverse Monte Carlo simulations

D. Le Messurier [a], V. Petkov [a,*], S.W. Martin [b], Youngsik Kim [b,1], Y. Ren [c]

[a] Department of Physics, Central Michigan University, Dow 203, Mount Pleasant, MI 48859, United States
[b] Department of Materials Science and Engineering, Iowa State University, Ames, IA 50010, United States
[c] Advanced Photon Source, Argonne National Laboratory, Argonne, IL 60439, United States

ARTICLE INFO

ABSTRACT

A high-energy X-ray diffraction study has been carried out on a series of $0.5Li_2S + 0.5[(1 - x)GeS_2 + xGeO_2]$ glasses with $x = 0.0, 0.1, 0.2, 0.4, 0.6$ and 0.8. Structure factors were measured to wave vectors as high as 30 $Å^{-1}$ resulting in atomic pair distribution functions with high real space resolution. The three dimensional atomic-scale structure of the glasses was modeled by reverse Monte Carlo simulations based on the diffraction data. Results from the simulations show that at the atomic-scale $0.5Li_2S + 0.5[(1 - x)GeS_2 + xGeO_2]$ glasses may be viewed as an assembly of independent chains of $(Li^+ {}^-S)_2GeS_{2/2}$ and $(Li^+ {}^-O)_2GeO_{2/2}$ tetrahedra as repeat units, where the Li ions occupy the open space between the chains. The new structure data may help understand the reasons for the sharp maximum in the Li^+ ion conductivity at $x \sim 0.2$.

© 2009 Elsevier B.V. All rights reserved.

1. Introduction

Sulfide glasses such as $LiI + Li_2S + P_2S_5$ [1], $LiI + Li_2S + B_2S_3$ [2], and $LiI + Li_2S + SiS_2$ [3] are well known for their high lithium ion conductivities, which are typically greater than $10^{-3} S\,cm^{-1}$ at room temperature. There is, however, a down side to LiI-doped glasses in that they are unstable in contact with high activity Li metals used as anode materials in solid-state batteries. This instability causes a decrease in the performance for lithium batteries that are fabricated using such glasses as solid electrolytes [4–7]. However, it has been reported that small amounts (typically less than 10–20 mole%) of lithium oxysalts, Li_xMO_y, (where Li_xMO_y is of the type Li_3PO_4, Li_4SiO_4, Li_3BO_3, and Li_4GeO_4), added to the base $Li_2S + SiS_2$ glass system increases the glass' stability towards Li metal and, in some favorable cases, actually improves their high ionic conductivity [7–9]. At higher additions of these lithium oxysalts, the lithium ion conductivity decreases as might be expected from the significantly lower lithium ion conductivity of oxide glasses compared to sulfide glasses [10].

Several studies have attempted to reveal the origin of the sharp maximum in the Li^+ ion conductivity at these relatively small amounts of dopant lithium oxysalt. Tatsumisago et al. [8] studied this effect in some detail but in the process introduced three simultaneous changes to the base sulfide glass, the addition of lithium oxysalts, the addition of oxygen, and in some cases the addition of a second so-called 'framework cation'. The complexity of these changes did not allow to reveal exactly which of them, and to what extent, caused the sharp maximum observed in the lithium ion conductivity.

The increased Li^+ ion conductivity has also been studied by Kim et al. [11] who explored a compositionally simpler system: $0.5Li_2S + 0.5[(1 - x)GeS_2 + xGeO_2]$, with $x = 0-1$, where the only substitution is that of sulfur with oxygen. A further simplifying aspect of this particular series of glasses is the fact that at $x = 0$ the atomic-scale structure of the pure thio-germanate glass, $0.5Li_2S + 0.5GeS_2$, consists of linear chains of Ge–S₄ tetrahedra [12], more formally given as $(Li^+ {}^-S)_2GeS_{2/2}$, with sulfur atoms

* Corresponding author.
  E-mail address: petkov@phy.cmich.edu (V. Petkov).
[1] Present address: 1 University Station, C2201, Texas Material Institute, University of Texas at Austin, Austin, TX 78712-0292, United States.
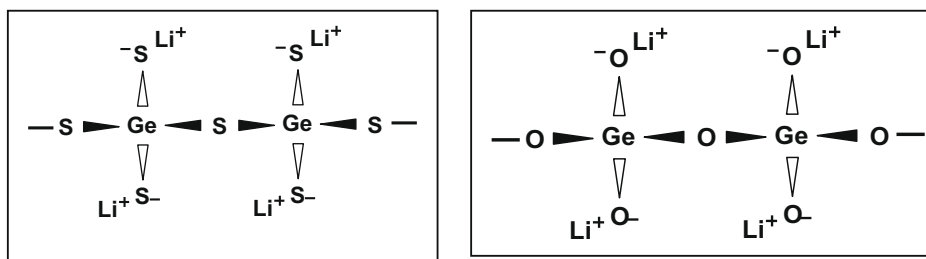
Fig. 1. Sketch of the linear chains of Ge–S_4 and Ge–O_4 tetrahedra occurring in pure thio- and oxy-germanate glasses, respectively. *Note*: sulfur and oxygen occur in both bridging and non-bridging positions. The former are coordinated with two Ge atoms and the latter with one Ge and one Li atom. The tetrahedra and the Li ions associated with them may be described by the following formula units: (Li$^+$ $^-$S)$_2$[GeS$_{2/2}$] and (Li$^+$ $^-$O)$_2$ [GeO$_{2/2}$], respectively. Here atoms in parentheses, (), are in NBP and atoms in square brackets, [], in BP.

occupying both non-bridging (NBP) and bridging (BP) positions and Li$^+$ ions occupying the open space between the chains as shown in Fig. 1. In the analogous pure oxy-germanate glass, $0.5Li_2O + 0.5GeO_2$ a similar atomic-scale structure is found with oxygen also occupying NBPs and BPs within linear chains of Ge–O_4 tetrahedra, again more formally given as (Li$^+$ $^-$O)$_2$GeO$_{2/2}$, as shown in Fig. 1. Therefore, in the 'mixed glasses' of composition $0.5Li_2S + 0.5[(1 − x)GeS_2 + xGeO_2]$, it could be expected that the added oxygen would enter into one of these two positions. Indeed Kim et al. suggested through their IR and Raman experiments [11] that initially the added oxygen replaced only sulfur in the BP in the chains of Ge-based tetrahedra up to the point that all BP sulfurs positions had been replaced by oxygen. Only after this composition, $x = 0.5$, the added oxygen started replacing NBP sulfur atoms.

While some understanding of the evolution of the atomic ordering in these relatively simple (from a compositional point of view) 'mixed glasses' with increasing oxygen content has been achieved, their three-dimensional structure has not been determined in full detail. Such knowledge is a prerequisite to understanding and, hence, better utilizing the effect of increased Li$^+$ ion conductivity. For this reason $0.5Li_2S + 0.5[(1 − x)GeS_2 + xGeO_2]$ glasses with $x = 0, 0.1, 0.2, 0.4, 0.6$ and 0.8 were subjected to a detailed structure study involving high-energy X-ray diffraction (XRD) and reverse Monte Carlo (RMC) simulations. Results from this study are reported below.

2. Experimental

2.1. Sample preparation

Vitreous GeS_2 was prepared by mixing and reacting Ge (Cerac, 99.999%) and S (Cerac, 99.999%) in an evacuated silica tube. The silica tube was held inside a furnace for 8 h at a temperature of 900 °C and then quenched in air. Ternary $Li_2S–GeS_2–GeO_2$ glasses were prepared by reacting stoichiometric amounts of LiS_2 (Cerac, 99.9%), GeS_2 and GeO_2 (Cerac, 99.999%) using a bulk melt and rapid quench technique. The starting materials were mixed and then placed in a covered vitreous carbon crucible and heated for 5–10 min between 850 and 1100 °C, depending on the particular composition. The crucible was held inside a tube furnace attached to the side of a nitrogen-filled glove box. The molten samples were quenched between two brass plates at room temperature. The glasses were generally transparent with a reddish or yellowish color.

2.2. High-energy X-ray diffraction experiments

X-ray diffraction experiments were carried out at the beam line 11IDC at the Advanced Photon Source using using X-rays with energy of 115.232 keV ($\lambda = 0.1076$ Å) and a large area (mar345

detector. Synchrotron radiation X-rays were used for two reasons. Firstly, the higher flux of synchrotron radiation X-rays makes it possible to measure the rather diffuse diffraction patterns of glasses with a very good statistical accuracy [13]. Secondly, the higher energy of synchrotron radiation X-rays makes it possible to reach high wave vectors, Q, resulting in atomic distribution functions with very good real space resolution [14]. Glasses were sealed in thin walled quartz capillaries and measured at room temperature. Up to ten exposures were taken for each of the samples, and each exposure lasted 15 min. A typical 2D diffraction pattern and a 1D data set extracted from it are given in Fig. 2. The experimental XRD data were reduced to structure factors, $S(Q)$, defined as follows:

$$S(Q) = 1 + \left[I^{el}(Q) − \Sigma c_i \mid f_i(Q)\mid^2\right] / \mid \Sigma c_i f_i(Q)\mid^2, \tag{1}$$

where c_i and f_i are the atomic concentration and scattering factor, respectively, for the atomic species of type i, (here i = Ge, O, S and Li), Q is the wave vector and $I^{el}(Q)$ the elastic component of the total diffracted intensities [14]. The experimental $S(Q)$ data are shown in Fig. 3 up to the maximum wave vector of 30 Å^{-1} reached in the present experiments. Experimental atomic PDFs $g(r) = \rho(r)/\rho_o$, where $\rho(r)$ and ρ_o are the local and average atomic number density, and r is the radial distance are shown in Fig. 4. Atomic PDFs were obtained by a Fourier transformation [15] of the experimental structure factors using Eq. (2):

$$g(r) = 1 + (1/(2\pi^2\rho_0 r)) \int_{Q=0}^{Q_{max}} Q[S(Q) − 1]\sin(Qr)\,dQ. \tag{2}$$

The extraction of $I^{el}(Q)$ from the raw diffraction intensities and derivation of the experimental PDFs was done with the help of the program RAD [16].

3. Results

Experimental PDFs peak at real space distances where frequent atomic pairs occur. The area under a PDF peak corresponds to the number of particular atomic pairs at that distance. As can be seen in Fig. 4, the peaks in the experimental PDFs for $0.5Li_2S + 0.5[(1 − x)GeS_2 + xGeO_2]$ glasses decay to zero for distances greater than 7–8 Å, a behavior typical for materials that lack long-range atomic ordering. As can also be seen in Fig. 4, the experimental PDFs show well-defined low-r peaks indicating that all of the glasses studied have a very well-defined short-range atomic order. In particular, the PDF $g(r)$ for the glass with $x = 0$ has its first peak positioned at 2.23(2) Å and the second at 3.65(5) Å. These are the interatomic distances between the first neighbor unlike, Ge–S, and like, S–S and Ge–Ge, atomic pairs found in corner sharing Ge–S_4 tetrahedra, more formerly given as (Li$^+$ $^-$S)$_2$GeS$_{2/2}$ [17]. Note that the PDF for the glass with $x = 0$ shows no physically sensible
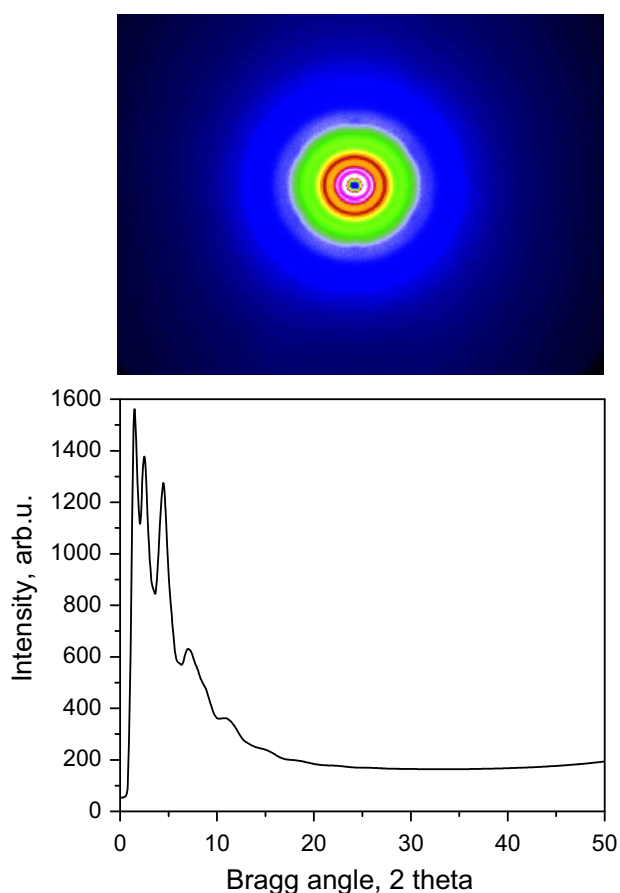
Fig. 2. 2D diffraction pattern for $0.5Li_2S + 0.5[(1 - x)GeS_2 + xGeO_2]$ glass with $x = 0$ (upper part) and 1D data set (lower part) extracted from it.

Fig. 4. Experimental atomic $g(r)$s for $0.5Li_2S + 0.5[(1 - x)GeS_2 + xGeO_2]$ glasses (lower part). Pairs of corner sharing Ge–S_4 and Ge–O_4 tetrahedra (Ge = grey, S = yellow, O = blue circles) are shown in the upper part of the graph together with some of the corresponding interatomic distances (*note*: Li atoms are not shown for the sake of clarity). Those distances appear as well-defined peaks in the experimental data. In particular, the first two peaks in the experimental $g(r)$'s reflect the first neighbor Ge–(S;O) distances as marked in the plot. A vertical line (in blue) shows the position of the $g(r)$ peaks reflecting first neighbor S–S and Ge–Ge atomic pairs from corner sharing Ge–S_4 tetrahedra. Another vertical line (in red) shows the position of the $g(r)$ peak reflecting first neighbor O–O and Ge–Ge pairs from corner sharing Ge–O_4 tetrahedra. (For interpretation of the references to colour in this figure legend, the reader is referred to the web version of this article.)

Interatomic distances like these are observed with well-defined Ge–O_4 tetrahedra, again more formerly given as $(Li^+ \; ^-O)_2GeO_{2/2}$ [18]. The former distance corresponds to unlike, Ge–O, and the latter to like, O–O and Ge–Ge, atomic pairs from such corner sharing units (see the upper part of Fig. 4). Also, the intensity of the new PDF peaks grows with the oxygen content while that of the peaks reflecting the Ge–S_4 units diminishes. Furthermore, there appear to be no new peaks, or shoulders on existing peaks, associated with O–S atomic pairs that would be expected across the edge of 'mixed' Ge–$(O/S)_4$ tetrahedra. These observations suggest that, when replacing sulfur, oxygen tends to form its own Ge–O_4 coordination units, so that mixed $0.5Li_2S + 0.5[(1 - x)GeS_2 + xGeO_2]$ glasses, $x > 0$, comprise both Ge–S_4 and Ge–O_4 tetrahedra. This initial conclusion was checked and confirmed by computer simulations as described and shown below.

Not only the short, but the immediate-range order in these glasses also changes with the oxygen content. The latter changes are clearly demonstrated by the behavior of the low-Q part of the experimental $S(Q)$ data. In particular, both the positions and the intensity of the first two $S(Q)$ peaks change monotonically with the oxygen content (see Fig. 3). More details of the short and medium-range atomic ordering in the glasses studied were revealed by reverse Monte Carlo simulations based on the experimental data.
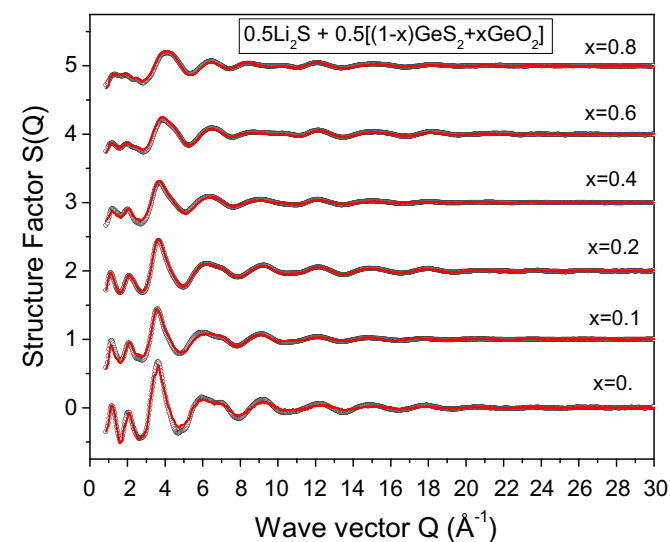

Fig. 3. Experimental (symbols) and Model III (line in red) structure factors $S(Q)$ for $0.5Li_2S + 0.5[(1 - x)GeS_2 + xGeO_2]$ glasses. (For interpretation of the references to colour in this figure legend, the reader is referred to the web version of this article.)

peaks below 2 Å and between 2.5–3.4 Å indicating, in line with the previous IR and Raman experiments [11], that this glass is built of only well-defined Ge–S_4 units.

Upon addition of oxygen, however, the short-range order in the glasses changes. New PDF peaks appear at 1.78(2) Å and 3.3(1) Å.
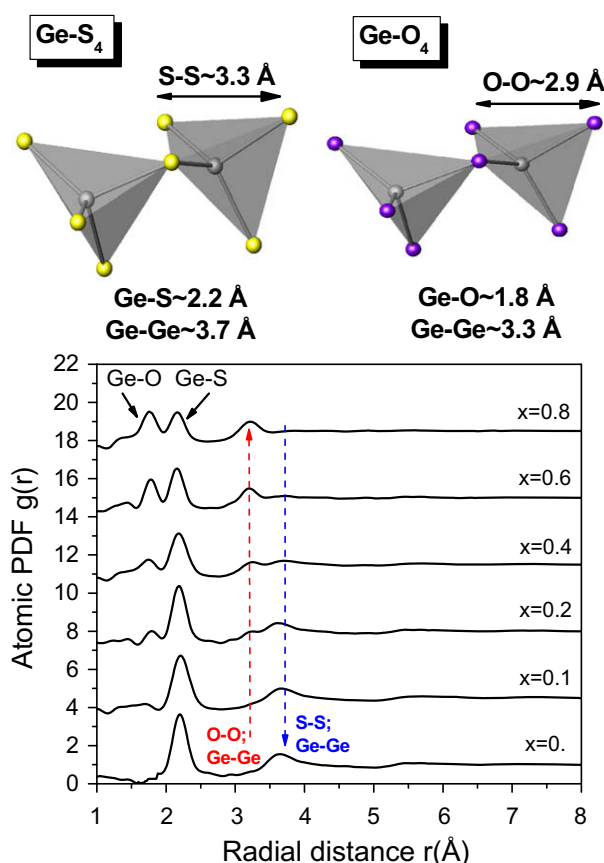
4. Modeling

Reverse Monte Carlo (RMC) simulations were employed to model the atomic-scale structure of $0.5Li_2S + 0.5[(1 - x)GeS_2 + xGeO_2]$ glasses [19]. The method involves building of atomic configurations in a simulation box and refining them against experimental, structure-sensitive data such as $S(Q)$ and $g(r)$'s. The refinement is done by varying the atomic coordinates in a random manner as to obtain the best possible agreement between the model computed and experimentally determined $S(Q)$ and $g(r)$'s within plausible structural constraints. Usually, the imposed constraints include the glass' chemical composition, density, distances of closest interatomic approach and first coordination numbers. At first we modeled the structure of the pure sulfide glass, $x = 0$, and then this model structure was modified to represent the stoichiometry of oxy-sulfide glasses, $x > 0$, by replacing an appropriate number of sulfur atoms with oxygen atoms. Different modes of 'replacement' were attempted: one featured oxygen occupying only NBPs (Model I), one featured oxygen occupying only BPs as suggested by Rao and Ganguli [10] (Model II) up until all sulfur atoms in BP had been occupied (Model II), and one featured oxygen in both NBPs and BPs in the glass network for all compositions x (Model III). Atoms in the configurations were moved until good agreement (e.g. goodness-of-fit factors of at least 5%) between the computed model and the experimental structure data, PDFs and $S(Q)$s, was achieved within several chemically and structurally-sensible constraints such as, for example, the presence of well-defined tetrahedral units.

4.1. Modeling the structure of the pure sulfide glass (x = 0)

Since the stoichiometry of Na_2GeS_3 crystal is similar to that of the $0.5Li_2S + 0.5[(1 - x)GeS_2 + xGeO_2]$ glass with $x = 0$, the structure of the former was used as a starting model for that of the latter. Crystalline Na_2GeS_3 may be viewed as an assembly of parallel chains of Ge–S_4 tetrahedra with alkali (Na) ions sitting between the chains where the repeat unit of the chains is given as $(Na^+ {}^-S)_2GeS_{2/2}$ [20]. Using the Na_2GeS_3 crystal structure as a starting configuration, and replacing Na for Li, it was possible to model the experimental diffraction data for the oxygen free glass ($x = 0.0$). The model consisted of 5000 atoms: Ge, S and Li, with the relevant proportions, densities, and atomic minimum approach distances shown in Tables 1–3, respectively. This success reinforced the conclusions of the preliminary analysis of the PDF data, namely, that the $0.5Li_2S + 0.5[(1 - x)GeS_2 + xGeO_2]$ glass with $x = 0$ is composed of linear chains of well-defined Ge–S_4 tetrahedra. In

Table 1
Number of atoms of each type used in the RMC simulations.

Atom type	$x = 0.0$	$x = 0.1$	$x = 0.2$	$x = 0.4$	$x = 0.6$	$x = 0.8$
Li	1665	1665	1665	1665	1665	1665
Ge	835	835	835	835	835	835
S	2500	2335	2175	1835	1500	1165
O	0	165	325	665	1000	1335

Table 2
Atomic number densities used in the RMC simulations.

Composition	Density (atoms/Å^{-3}) ± 0.0001
$x = 0.0$	0.0484
$x = 0.1$	0.0495
$x = 0.2$	0.0508
$x = 0.4$	0.0550
$x = 0.6$	0.0603
$x = 0.8$	0.0649

Table 3
Distances of closest interatomic approach (also known as 'cut-off lengths') used in the RMC simulations.

Atomic pairs	Cut-off length, Å
Li–Li	2.3
Li–Ge	2.2
Li–S	2.0
Li–O	1.7
Ge–Ge	3.3
Ge–S	1.9
Ge–O	1.5
S–S	3.0
S–O	3.0
O–O	2.7

this structure model sulfur atoms occupy both NBPs and BPs in the proportion 1:1 as shown in Fig. 1. Within this notation the basic structural unit of the glass may be denoted as $(Li^+ {}^-S)_2[GeS_{2/2}]$, where atoms in parentheses, (), are in NBPs and atoms in square brackets, [], in BPs, respectively.

### 4.2. Modeling the structure of oxy-sulfide glasses (x > 0): Model I: oxygen in NBPs only

To explore the structure of 'oxy-sulfide' glasses the first and simplest model we attempted was the case of oxygen atoms occupying NBPs only. This was done in the following way: for each of the compositions studied an appropriate number of Ge–S_4 tetrahedra from the model structure of the glass with $x = 0$ were selected at random and all of their sulfur atoms replaced with oxygen atoms. Bond length constraints were then placed on these new oxygen-based tetrahedra and the system allowed to structurally relax in its new state. Following this procedure experimental XRD data was then added to further constrain the model. Relatively good agreement between the model and experimental data was achieved except for the first $g(r)$ peak. As an example a comparison between the experimental and model calculated $g(r)$ for the glass with $x = 0.4$ is shown in Fig. 5(a). As can be seen in the figure the first peak in the model $g(r)$ is lower in intensity than that in the experimental $g(r)$ indicating a 'deficiency' of Ge–O bonds in the model atomic configuration.

This problem stems from the fact that thus created Ge–O_4 tetrahedra remained largely isolated from each other resulting in all oxygen atoms having just one Ge atom as a first neighbor. In a configuration where Ge–O_4 tetrahedra share their vertices (see Figs. 1 and 3) some oxygen atoms would occupy BPs and, hence, have two Ge atoms as first neighbors that would lead to a larger number of Ge–O bonds. Furthermore, the formation of isolated Ge–O_4 tetrahedra at the expense of Ge–S_4 ones connected in chains would be expected to break up the glass network. At higher oxygen contents this breakup would be very substantial and would result in a reduction of the viscosity of the glass that should be seen as a lowering in the glass transition temperature, T_g. However, this is not seen in the T_gs as measured by us [21]. These inconsistencies suggest that Model I featuring isolated Ge–O_4 and chains of corner shared Ge–S_4 tetrahedra, i.e. a mixture of $(Li^+ {}^-O)_4Ge$ and $(Li^+ {}^-S)_2[GeS_{2/2}]$ units, is inappropriate for describing the oxy-sulfide members of the glass system studied.

4.3. Model (II): oxygen in BPs only

Again the model for the pure sulfide glass was used as a starting point, for the reasons outlined above. For the compositions containing oxygen, sulfur atoms in BPs (i.e. Ge–S–Ge) were replaced in an random manner throughout the configuration by oxygen atoms both to reproduce the correct composition and to keep the
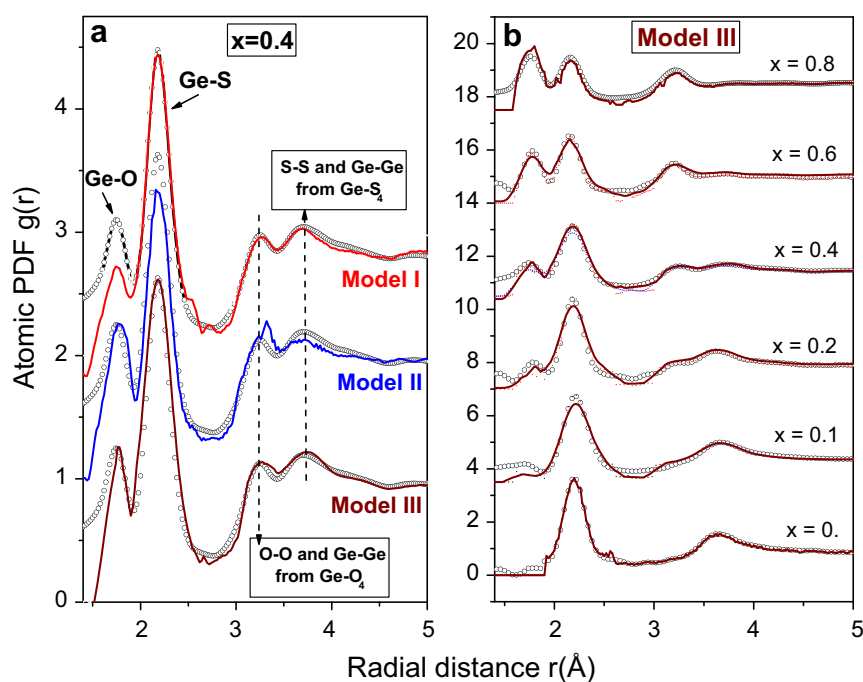
Fig. 5. Low-r part of the experimental (symbols) and model (lines in color) atomic $g(r)$s for $0.5Li_2S + 0.5[(1 − x)GeS_2 + xGeO_2]$ glass with $x = 0.4$. The $g(r)$ peaks are labeled with the corresponding atomic pairs (a). Low-r part of the experimental (symbols) $g(r)$s for $0.5Li_2S + 0.5[(1 − x)GeS_2 + xGeO_2]$ glasses. The experimental data are compared to model $g(r)$s (line) computed on the basis of Model III. (For interpretation of the references to colour in this figure legend, the reader is referred to the web version of this article.)

connectivity of the glass network (and the number of Ge–O bonds) as high as possible as described by Rao and Ganguli [10]. Length constraints were then placed on these new oxygen-involving bonds (see Table 3) and the system allowed to structurally relax in its new state Accordingly, for $0 < x < 0.5$, the model atomic configurations consisted of chains of 'mixed' Ge–(S/O)$_4$ tetrahedra having oxygen at BPs and sulfur at both BPs and NBPs, in addition to the chains of Ge–S$_4$ tetrahedra originally present in the starting atomic configuration. For $x > 0.5$, the oxygen occupied all of the BPs and some of the NBPs in the chains of 'mixed' tetrahedra. Overall, with increasing oxygen the length of chains of tetrahedra having both oxygen and sulfur on their vertices, i.e. chains of (Li$^+$ $^-$S)$_2$[GeO$_x$S$_{2−x}$] units, increased and that of the chains of only Ge–S$_4$ tetrahedra, i.e. chains of (Li$^+$ $^-$S)$_2$[GeS$_{2/2}$] units, decreased. This model was able to reproduce well the first peak (i.e. the number of Ge–O bonds) in the experimental data but failed to reproduce well the subsequent two $g(r)$ peaks as exemplified in Fig. 5(a). The disagreement shows that the preferential replacement of bridging sulfur atoms by oxygen converts too many of the original Ge–S$_4$ tetrahedra into 'mixed' Ge–(S/O)$_4$ ones leading to a deficiency in the Ge–S, S–S and Ge–Ge bonds from the former units. The deficiency is seen as misfit between the experimental and model data in the vicinity of the respective $g(r)$ peaks at $2.23(2)$ Å and $3.65(5)$ Å, as shown in Fig. 5(a). The misfit showed that this model was not quite appropriate to describe the structure of the 'oxy-sulfide' glasses, as probed by high-energy XRD, either.

4.4. Model (III): oxygen in both BPs and NBPs

Taking into account the outcomes of the first two unsuccessful attempts we constructed a third model featuring a random network of independent chains of Ge–O$_4$ and Ge–S$_4$ tetrahedra, i.e. a glass structure model where oxygen, like sulfur, occupies both NBPs and BPs for any $x > 0$. The chains comprised of either Ge–O$_4$ or Ge–S$_4$ tetrahedra, i.e. either (Li$^+$ $^-$S)$_2$[GeS$_{2/2}$] or (Li$^+$ $^-$O)$_2$[GeO$_{2/2}$] units, which allowed the connectivity of the glass network to be

kept high and the number of 'mixed' Ge–(S/O)$_4$ tetrahedra low. Upon increasing the oxygen content the length of the chains of Ge–S$_4$ decreased and that of the chains of Ge–O$_4$ tetrahedra increased accordingly. The model consisted of 5000 atoms: Ge, S, O and Li. The proportions of atoms used with the different glass compositions are shown in Table 1, the associated atomic densities in Table 2, and the cut-off values, i.e. distances of closest approach between the atoms in the model configuration, in Table 3. During the refinement, constraints were placed on the intra-tetrahedral angles to be close to ~110°, the relative number of BP atoms to be close to
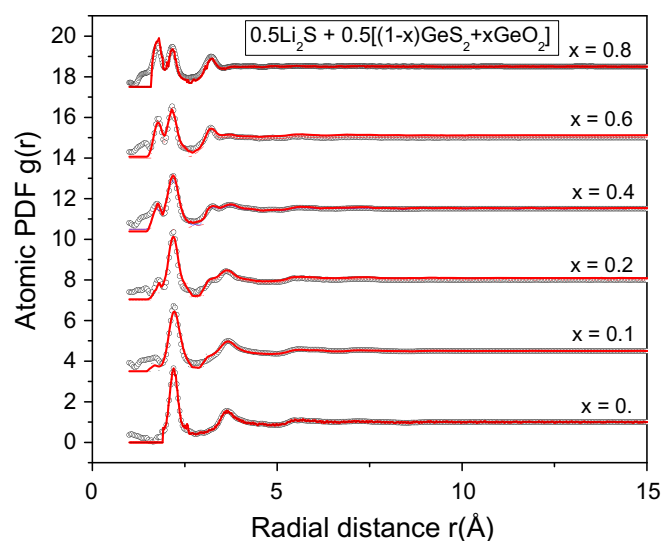

Fig. 6. Experimental (symbols) and Model III (line in red) $g(r) = \rho(r)/\rho_o$ for $0.5Li_2S + 0.5[(1 − x)GeS_2 + xGeO_2]$ glasses. The model $g(r)$'s are computed by reverse Monte Carlo simulations as explained in the text. (For interpretation of the references to colour in this figure legend, the reader is referred to the web version of this article.)

33% and that for NBP atoms to be close to 66%, and the Ge–O and Ge–S bond lengths to fall within 1.5–1.9 Å and 1.9–2.6 Å, respectively. The inter-tetrahedral angle, the angle between the corner sharing tetrahedra, was allowed to evolve freely. This model best reproduced the experimental $g(r)$ data as can be seen in Fig. 5(a), where all three models are applied to the same glass with an intermediate value of x, $x = 0.4$. Also, it was able to reproduce the experimental data for the other glasses reasonably well as can be seen in Fig. 5(b). For this reason, Model III was explored to the fullest extent by refining it to fit the experimental diffraction data for all $0.5Li_2S + 0.5[(1 − x)GeS_2 + xGeO_2]$ glass in both real and reciprocal spaces. The model refinement in both reciprocal and real space was necessary since in the former the structure factor data showed strong low-Q features that emphasize the medium-range order, while in the latter the atomic pair distribution function data showed well-defined low-r features that emphasize the short-range atomic order in the $0.5Li_2S + 0.5[(1 − x)GeS_2 + xGeO_2]$ glasses studied. A realistic structure model should reflect well both their short and the medium-range atomic ordering since both substantially affect the glass' property we are interested in, namely the conductivity of Li^+ ions.

5. Discussion

Results of the RMC simulations based on Model III are shown in Figs. 3 and 6, respectively. As can be seen in Fig. 3, there is very good agreement between the model and experimental structure factors. As can be seen in Fig. 6, the agreement between the model and experimental data is very good in real space as well. In particular, the model $g(r)$s reproduce the growth in the peak located at 1.78(2) Å, reflecting the Ge–O bonds from the Ge–O_4 tetrahedra, and the decrease in the intensity of the peak located at 2.23(2) Å, reflecting the Ge–S bonds from the Ge–S_4 tetrahedra. The $g(r)$ peaks reflecting the correlations between the like O–O and Ge–Ge, and S–S and Ge–Ge atomic pairs from the corner sharing Ge–O_4 and Ge–S_4 tetrahedra, respectively, (see Fig. 4, the upper part)
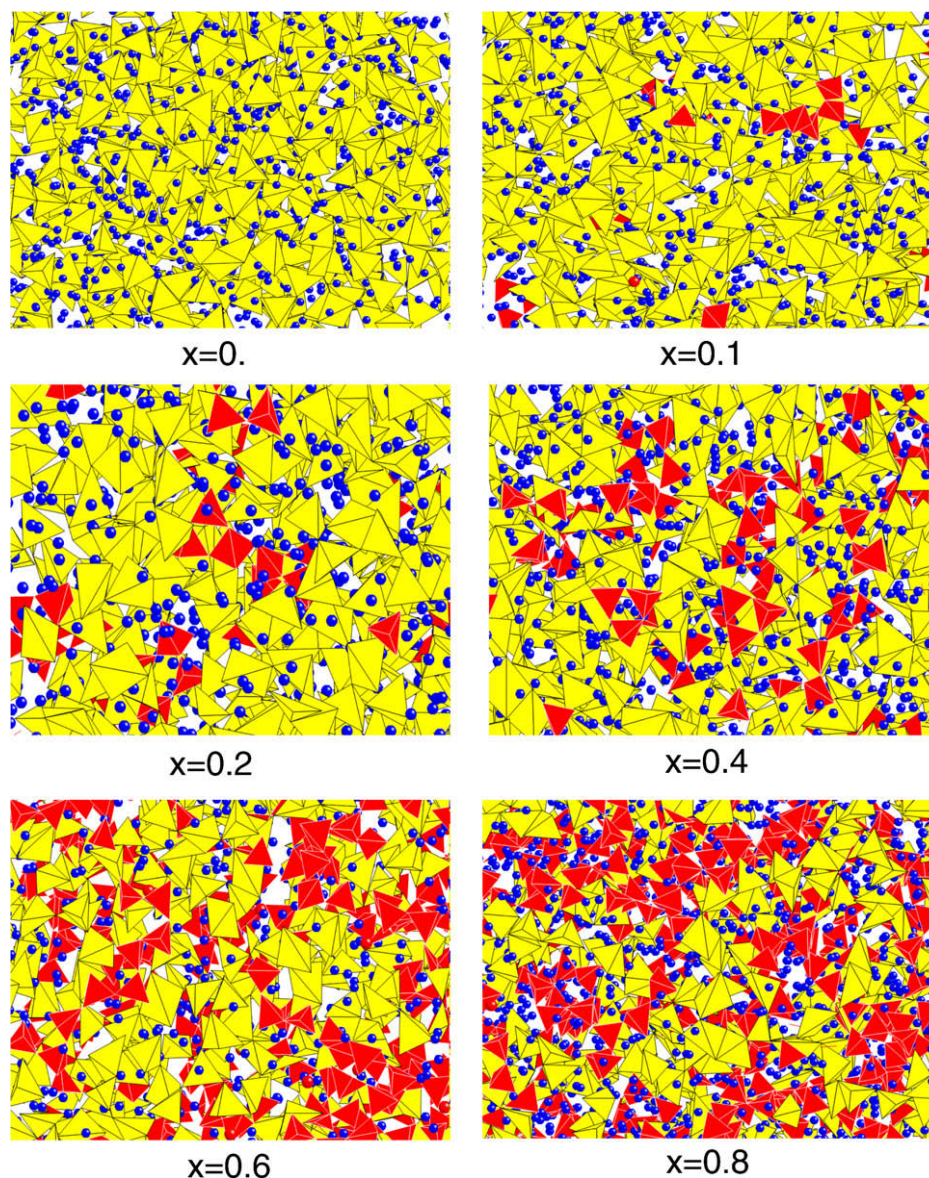
Fig. 7. Fragments from the RMC generated structure Model III for $0.5Li_2S + 0.5[(1−x)GeS_2 + xGeO_2]$ glasses. Ge–S_4 tetrahedra (yellow), Ge–O_4 tetrahedra (red), Li atoms (blue). Structure models feature network of chains of Ge–S_4 at $x = 0.0$ that gradually transforms into a network of independent chains of Ge–S_4 and Ge–O_4 tetrahedra with increasing oxygen content. The distribution of Li atoms inside the network cavities remains quite uniform throughout the series of glasses studied. (For interpretation of the references to colour in this figure legend, the reader is referred to the web version of this article.)

are also reproduced very well. The discrepancies in the agreement below distances of 1.5 Å are due to the minimum cut-off distances used in the modeling procedure and to the usual presence of some experimental errors that tend to pile up at low-*r* values. The small discrepancies in the Ge–O peak of compositions where *x* = 0.1 and *x* = 0.2 are due to the small amount of oxygen in the system. An improvement in the fits may be achieved by a slight adjustment of the number of oxygen atoms in the model system.

Fragments of the structural models generated by RMC simulations are shown in Fig. 7. As can be seen in the figure, the addition of more oxygen to the random network of chains of Ge–S$_4$ tetrahedra changes it into a random network of independent chains of Ge–S$_4$ and Ge–O$_4$ tetrahedra. At the same time, the distribution of Li atoms inside the network cavities remains more or less uniform. Thus, according to our modeling studies the 'oxy-sulfide' 0.5Li$_2$S + 0.5[(1 − *x*)GeS$_2$ + *x*GeO$_2$] glasses are comprised of two glass former anions, oxygen and sulfur, that keep their usual coordination environment, creating well-defined (Li$^+$ $^-$S)$_2$[GeS$_{2/2}$] and (Li$^+$ $^-$O)$_2$[GeO$_{2/2}$] units, for all *x*. This conclusion is confirmed by an analysis of the model atomic configuration showing that Ge–O and Ge–S bond lengths remain almost the same across the compositional range studied: approximately 1.78(2) Å and 2.23(2) Å, respectively.

First neighbor Ge–S and Ge–O coordination numbers are 3.9(1), a value typical for tetrahedral coordination. The small deviation of the computed first coordination numbers from the ideal number of four is due to 'edge' effects in the simulation box. The distribution of bond angles within the first Ge–O and Ge–S coordination spheres are shown in Fig. 8. The distribution of O–Ge–O bond angles remain constant through all compositions, with a modal value

of ~107°. There is, however, a change in S–Ge–S bond angle distribution with the addition of oxygen atoms. For the *x* = 0.0 glass, the bond angles peak at ~104°. With increasing oxygen content, the distributions broadens and appears shifted to lower angles with a modal value of 98°. The small change in the S–Ge–S bond angle distribution with increasing oxygen content indicates that Ge–S$_4$ tetrahedra distort somewhat, while keeping the average Ge–S bond constant. A possible reason for the distortion in the Ge–S$_4$ tetrahedra could be the emergence of Ge–O$_4$ units that are known to be more rigid than the Ge–S$_4$ ones [22]. The deformation in Ge–S$_4$ units allow the glass structure to rearrange, creating space for the Ge–O$_4$ ones. The evolution of this process may be traced in Fig. 7. Also, it is seen as a gradual re-distribution of the Ge–Ge correlations, i.e. of the way the chains of Ge-based tetrahedra fill up the space (see the Ge–Ge partial distribution functions shown in Fig. 9).

Although the distribution of Li atoms inside the network cavities remains quite uniform, the coordination environment of Li atoms changes across this series of glasses as demonstrated by the Li–O and Li–S partial distribution functions shown in Fig. 9. If one considers that the immediate coordination environment of Li extends to about 3.5 Å, then it comprises about four sulfur atoms in the glass with *x* = 0. In the glass with *x* = 0.8, the Li atoms have, on average, 2.5 sulfur and three oxygen atoms within the same coordination distance (see Fig. 10). The changes in the coordination environment of mobile Li ions will definitely affect the energy landscape around them since oxygen and sulfur have different electronic configurations. Indeed, a mechanism explaining how the substitution of sulfur by oxygen in the Li ion first coordination sphere may cause an abrupt and favorable increase in the Li ion
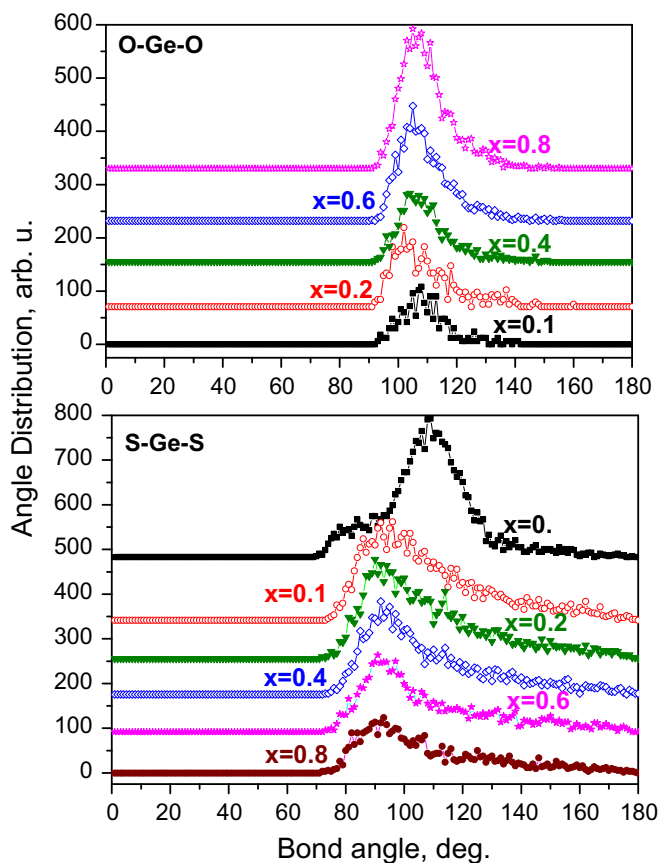

Fig. 8. Oxygen–Ge–oxygen and sulfur–Ge–sulfur bond angle distributions in the RMC generated structure Model III for 0.5Li$_2$S + 0.5[(1 − *x*)GeS$_2$ + *x*GeO$_2$] glasses. The distributions are shifted upward for clarity.
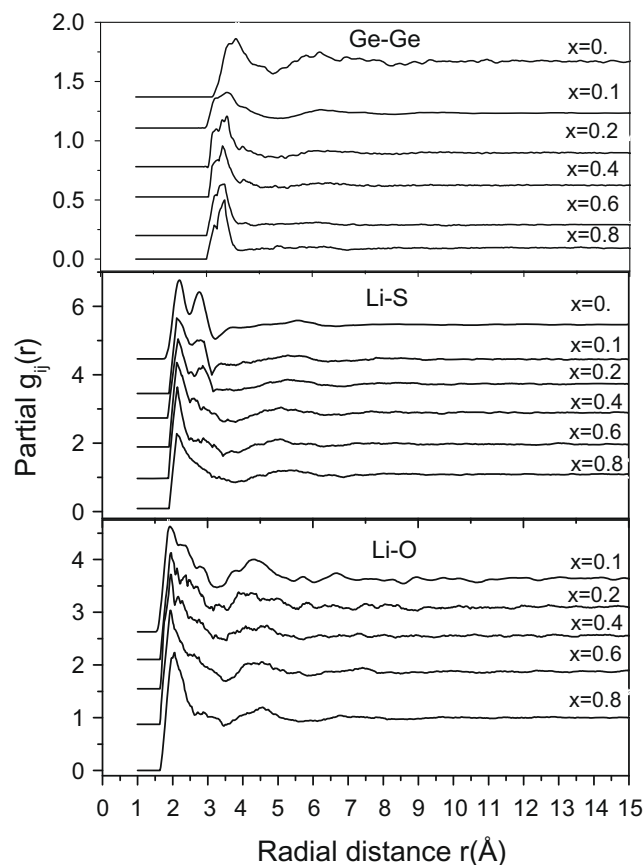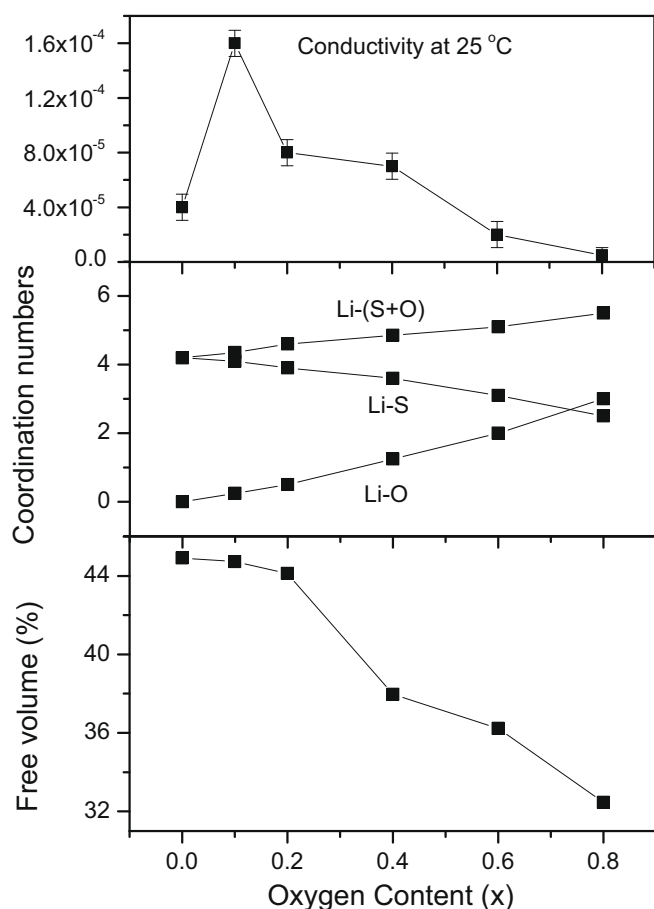

Fig. 9. Selected partial atomic distribution functions $g_{ij}(r)$ for 0.5Li$_2$S + 0.5[(1 − *x*)-GeS$_2$ + *x*GeO$_2$] glasses computed from the RMC generated structure Model III.

Fig. 10. Conductivity (in S cm^{-1}), Li first coordination numbers and volume available to the mobile ions (Li$^+$) in $0.5Li_2S + 0.5[(1 − x)GeS_2 + xGeO_2]$ glasses.

conductivity in $0.5Li_2S + 0.5[(1 − x)GeS_2 + xGeO_2]$ glasses has already been discussed by Rao and Ganguli [10].

The free volume, i.e. the volume not occupied by Ge–O$_4$ and Ge–S$_4$ tetrahedra in the glasses, also changes with increasing oxygen content. It is seen to decrease steadily, see Fig. 10, reflecting the densification of the glasses, see Table 2. A similar trend has been reported by Kim et al. [11].

Finally, the ionic conductivity in the $0.5Li_2S + 0.5[(1 − x)GeS_2 + xGeO_2]$ glasses is also shown in Fig. 10. It is seen to increase markedly at an oxygen concentration of $x \sim 0.2$ and then decrease. The ionic conductivity in the glasses studied would depend strongly on the medium-range order characteristics of the glass network such as the distribution and volume of free space available to mobile Li ions. Also, it would depend strongly on the short-range order characteristics of the glass network such as the chemical type of the Li coordination environment, i.e. on the type of electrostatic interactions of Li with its immediate environment inside the network of Ge–S$_4$ and Ge–O$_4$ tetrahedra. Since both the distribution of free volume occupied by Li ions, e.g. see the change in Ge–Ge correlations, and their chemical environment, e.g. see the variation in the Li first coordination numbers, change in the glasses investigated, it is not surprising that their conductivity may change significantly regardless of the fact that the concentration of mobile Li ions remains constant.

6. Conclusions

High-energy XRD has been used to study $0.5Li_2S + 0.5[(1 − x)GeS_2 + xGeO_2]$ glasses with $x = 0$, 0.1, 0.2, 0.4, 0.6 and 0.8. The XRD data has been used as a basis for RMC simulations of the structure of these glasses. Experiments and simulations suggest that the glasses studied are composed of independent chains of Ge–S$_4$ and Ge–O$_4$ tetrahedra, with Li atoms occupying the open space between them creating chains of (Li$^+$ $^-$S)$_2$[GeS$_{2/2}$] and (Li$^+$ $^-$O)$_2$[GeO$_{2/2}$] units. This model picture disagrees somewhat with the findings of Rao and Ganguli [10] suggesting the presence of 'mixed' Ge–(S/O)$_4$ units for $x < 0.5$. The reasons for this disagreement are not well understood at present, and may require extra studies, such as neutron diffraction, to be clarified. Nevertheless, the 3D model atomic configurations constructed here allow important structural characteristics of $0.5Li_2S + 0.5[(1 − x)GeS_2 + xGeO_2]$ glasses to be assessed. For example, we find that the Ge-backbone of tetrahedral networks evolves, i.e. the free volume redistributes, and the number of oxygen and sulfur atoms in the immediate neighborhood of Li changes substantially with increasing oxygen content. Currently our efforts are focused on revealing the interplay between these structural changes and the marked increase in the Li$^+$ ion conductivity observed at about $x \sim 0.2$. Results will be reported in a subsequent paper.

Acknowledgements

References

[1] R. Mercier, J.P. Malugani, B. Fahys, A. Saida, Solid State Ionics 5 (1981) 663.
[2] H. Wada, M. Menetrier, A. Levasseur, P. Hagenmuller, Mater. Res. Bull. 18 (1981) 189.
[3] J. Kennedy, Y. Yang, J. Solid Sate Chem. 69 (1987) 252.
[4] S. Kondo, K. Takada, Y. Yamamura, Solid State Ionics 53–56 (1992) 1183.
[5] K. Takada, N. Aotani, S. Kondo, J. Power Sources 43&44 (1993) 135.
[6] J.H. Kennedy, Z. Zhang, Solid State Ionics 28–30 (1988) 726.
[7] Y. Yamamura, M. Hasegawa, K. Takada, S. Kondo, European Patent Application, EP 469574, 1992.
[8] M. Tatsumisago, K. Hirai, T. Hirata, M. Takahashi, T. Minami, Solid State Ionics 86–88 (1996) 487.
[9] A. Hayashi, H. Yamashita, M. Tatsumisago, T. Minami, Solid State Ionics 148 (2002) 381.
[10] K.J. Rao, M. Ganguli, Lithium ion conducting glasses, in: Handbook of Solid State Batteries Capacitors, 1995, p. 189.
[11] Y. Kim, J. Saienga, S.W. Martin, J. Phys. Chem. B 10 (33) (2006) 16318.
[12] A. Pradel, C. Rau, D. Bittencourt, P. Armand, E. Philippot, M. Ribes, Chem. Mater. 10 (1998) 2162.
[13] V. Petkov, D. Qadir, S. Shastri, Solid State Commun. 129 (2004) 239.
[14] V. Petkov, S.J.L. Billinge, S. Shastri, B. Himmel, Phys. Rev. Lett. 85 (2000) 3436.
[15] C.N.J. Wagner, J. Non-Cryst. Solids 31 (1978) 1.
[16] V. Petkov, J. Appl. Crystallogr. 22 (1989) 387.
[17] P. Salmon et al., J. Non-Cryst. Solids 293–295 (2001) 169.
[18] M. Micoulant, L. Cormier, G.S. Henderson, J. Phys.: Condens. Mat. 18 (2006) R753.
[19] M.T. Dove, M.G. Tucer, S.A. Wells, D.A. Keen, EMU Notes in Mineralogy 4 (2002) 59;
O. Gereben, P. Jovari, L. Temleitner, L. Pusztai, J. Optoelectron. Adv. Mater. 9 (2007) 3021.
[20] J. Olivier-Fourcade, E. Philippot, M. Ribes, M. Maurin, C.R. Seances Acad. Sci., Ser. C 274 (1972) 1185.
[21] Y. Kim, J. Saienga, S.W. Martin, J. Non-Cryst. Solids 351 (2005) 3716.
[22] G. Lucovsky, T. Mowrer, L.S. Sremaniak, J.L. Whitten, J. Non-Cryst. Solids 338–340 (2004) 155.